Available online at www.sciencedirect.com
SCIENCE DIRECT®
ELSEVIER
Nuclear Instruments and Methods in Physics Research A 557 (2006) 268–271
NUCLEAR INSTRUMENTS & METHODS IN PHYSICS RESEARCH Section A
www.elsevier.com/locate/nima

Characterization of ferrites at low temperature and high frequency

Valery Shemelin*, Matthias Liepe, Hasan Padamsee

Laboratory for Elementary-Particle Physics, Cornell University, Ithaca, NY 14853, USA

Available online 16 November 2005

Abstract

Complex values of dielectric permittivity and magnetic permeability of 10 different materials, ferrites and ceramics, are measured in a frequency range from 1 to 40 GHz at room temperature and at 80 K. Recommendations are done for material usage in a cryogenic load for higher-order modes in the superconducting RF cavities of the Energy Recovery Linac.

PACS: 29.17.+w; 42.25.Bs; 52.25.Sw

Keywords: Energy recovery; Higher-order modes; Absorption of RF radiation; Materials at low temperatures

1. Introduction

In high current storage rings with superconducting cavities, strong broadband higher-order mode (HOM) damping has been achieved by using beam-pipe ferrite loads, located at room temperature [1]. Adopting the same damping concept for the Energy Recovery Linac (ERL) with RF absorbers between the cavities in a cavity string will require operating the absorbers at a temperature of about 80 K. This temperature is high enough to intercept HOM power with good cryogenic efficiency, and is low enough to simplify the thermal transition to the cavities at 2 K. However, the electromagnetic properties of possible absorber materials were not well known at cryogenic temperatures. Therefore, we performed a measurement program at Cornell University to find possible absorbers for HOMs in the ERL. First results for ferrites TT2-111R, HexM3 and HexMZ in the frequency range from 1 to 17 GHz were presented earlier [2,3]. Now we have results of measurements for 10 different materials up to 40 GHz.

2. Materials

We examined materials listed in Table 1. Not all of them were measured in the whole frequency range because of absence of some samples with the necessary shape; they are marked by "minus" (−) in the table. Some materials appeared to be very brittle (C48-E1, C48-E2) and cannot be recommended for further usage in our project.

The tested materials fall into three groups: ferrites TT2-111R, C48-E1, C48-E2, hexagonal phase ferrites M1, M2, M3, and MZ [4,5], and Ceradyne ceramics ZR10CB5, ZR20CB5, Z7YL [6,7].

3. Measurements

The measurement procedure is described in Refs. [2,3]. For measurements of *S*-parameters in the region 12.4–40 GHz the network analyzer Agilent E8363B was used. So, the whole range from 1 to 40 GHz was covered by measurements with a coaxial line (7/3.05 mm, 1–15 GHz, HP8720 network analyzer), and with waveguides: WR62 (12.4–18 GHz), WR42 (18–26.5 GHz), and WR28 (26.5–40 GHz). Transmission lines used for measurements and samples to be measured are shown in Fig. 1.

We used the through, reflect, line (TRL) calibration as giving the most accurate results of measurements.

A schematic of the measurement is shown in Fig. 2. A coaxial line or two long waveguides with a short waveguide section between them were used. Shorter waveguide, with a sample, helped to decrease the errors related to evaluation of the phase shift for the complex *S*-parameters at higher frequencies. Reproducibility of the results was improved

*Corresponding author. Tel.: +1 607 255 5731; fax: +1 607 254 4552.
E-mail address: vs65@cornell.edu (V. Shemelin).

0168-9002/$ - see front matter © 2005 Elsevier B.V. All rights reserved.
doi:10.1016/j.nima.2005.10.081

Table 1
Materials and frequency ranges where they were measured

Material	Freq. (GHz)			
	1–12.4	12.4–18	18–26.5	26.5–40
TT2-111R	+	+	+	+
C48-E1	+	–	+	+
C48-E2	+	–	+	+
HexM1	+	+	+	+
HexM2	+	+	+	+
HexM3	+	+	+	+
HexMZ	+	+	+	+
ZR10CB5	–	+	+	+
ZR20CB5	–	+	+	+
Z7YL	–	+	+	+

Fig. 1. Transmission lines for four frequency ranges.

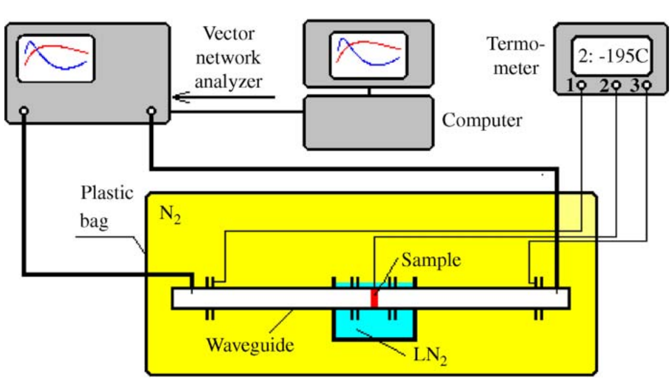

Fig. 2. Schematic of test setup.

when the connecting bolts were tightened with a torque wrench (10 or 15 N m). To improve the contraction after cooling, spring washers were used. The thickness of the used samples was less than half-wave length in the material, to avoid the resonance and decrease errors. Calibration of the analyzer before measurements of cold samples was also performed with cold waveguides joined to warmer adapters with coaxial cables connected to the analyzer. So, the procedure of calibration became more complicated because we needed three times cool down and then warm up of the waveguide line for changing calibration standards. Though the changes of the line length and of the dielectric constant of N_2 (data for air were used) partly compensated each other at 80 K, in a definition of the phase advance both effects should be taken into account especially for the long coaxial line. The position of the sample in the line, "insertion distance", was defined by numerical comparison of the complex reflections from each side: S_{11} and S_{22}. Before cooling, the waveguides were blown through with nitrogen and the experiment was housed under positive pressure of nitrogen atmosphere (inside a plastic bag) to prevent ice formation on the cooled parts (water has $\varepsilon \approx 80$!). Only the central part of the waveguide line with a cooled short waveguide was immersed into the bath with liquid nitrogen. Small holes in the waveguides were needed because, when being cooled down, the pressure in them drops more than a half of atmosphere, and, if leakage is uncontrolled, the sample moves in the waveguide like a piston. The temperature of the central part (that was about 78–80 K) and of the waveguide ends (190–200 K) was checked by thermocouple thermometers.

Temperature equilibrium was assumed to be achieved in 15 min after the start of cooling. The measured *S*-parameters were converted to complex ε and μ values following the algorithm outlined by Hartung [8].

4. Results

We present here only a small part of obtained results (Fig. 3) because of the lack of space; more data were presented on the transparencies [9]. The imaginary parts of both ε and μ should be negative, this means that material absorbs, not gives off, power. If our results show positive $\mathrm{Im}\,\varepsilon$ or $\mathrm{Im}\,\mu$, this indicates the limits of our accuracy only. The level of accuracy can be also seen from the deviation of $\mathrm{Im}\,\mu$ from 0 or $\mathrm{Re}\,\mu$ from 1 in Ceradynes measurements. Some data do not join together at the ends of frequency ranges. This can be related not with the errors of measurements only but with the difference of material properties for different batches of materials. Such a behavior was observed in data by Dohlus [7] for Zr20CB5 and for other materials from the DESY group at room temperature. Some errors can be caused by irregular shape of samples; it is hard to keep the right shape and small gaps between samples and waveguide walls for so small sizes. The influence of these shape deviations is planned to be studied on computer models.

A simplified absorption model for a plane wave has been calculated for a 3 mm thick absorber, see Fig. 4. The measured ε and μ data have been used as input for this

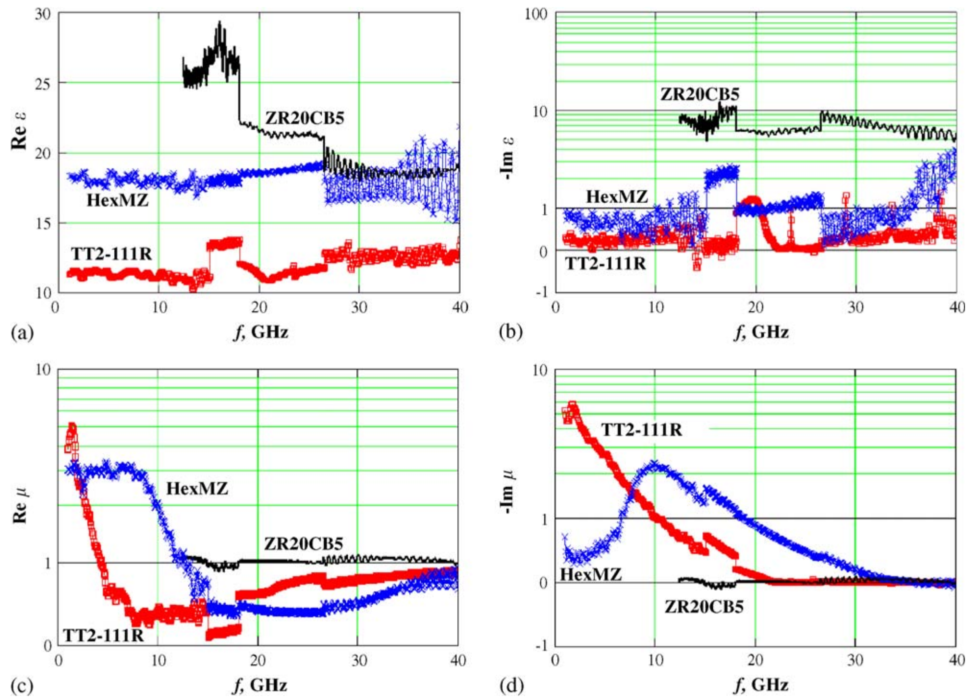

Fig. 3. Real and imaginary parts of ε and μ for three materials from 1 to 40 GHz at 80 K. The ordinate scale is logarithmic for values more than 1 and linear otherwise.

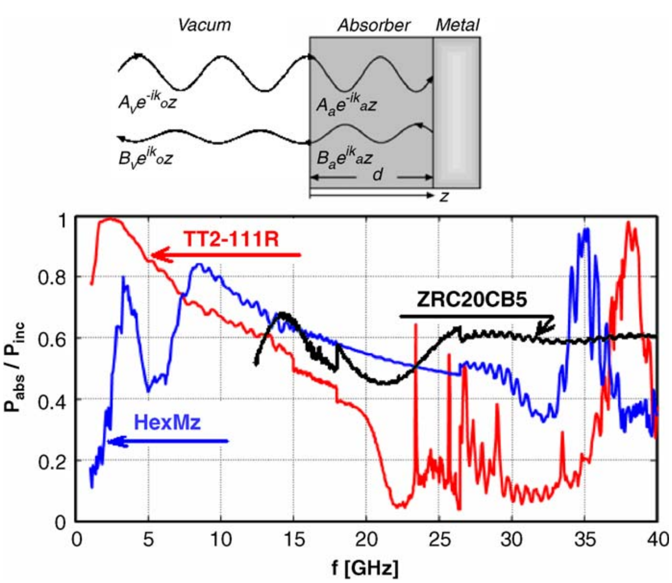

Fig. 4. Absorber model calculation ($d = 3$ mm) based on measured ε and μ at 80 K.

model. Peaks of absorption at 35 and 38 GHz are related to resonant thickness of the layer, not to the peaks of ε or μ. Real geometry of the absorber will be more complicated.

5. Conclusion

Several different materials have been evaluated with respect to the use as HOM absorbers for ERLs, and the most promising are presented here. Ferrite TT2-111R can be proposed as an absorber at 80 K in the lower part of the frequency range, and ceramics like ZR20CB5 can work at higher frequencies (Fig. 5). Ferrite HexMZ can work in the middle and higher frequencies. In the frequencies 15–30 GHz, both HexMZ and ZR20CB5 will complement each other because the losses in them are magnetic and electric, respectively. This should help to suppress different types of HOMs.

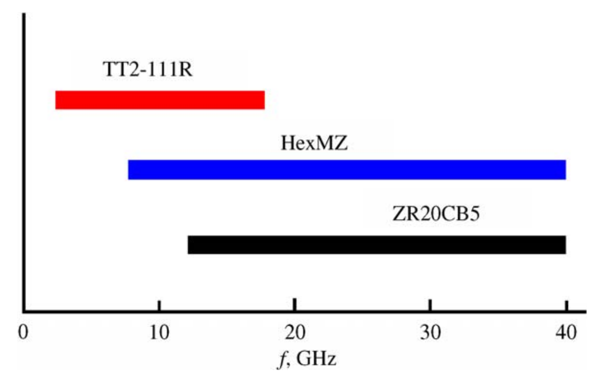

Fig. 5. Regions of application for three chosen materials.

Acknowledgments

We thank Martin Dohlus from DESY for providing Ceradyne samples and our colleagues from LEPP for help.

References

[1] D. Moffat, et al., in: Proceedings of the 1993 Particle Accelerators Conference, Washington, DC, 1993. p. 977.
[2] M. Liepe, B. Barstow, H. Padamsee, First studies for a low temperature higher-order-mode absorber for the Cornell ERL prototype, in: Proceedings of the 2003 Particle Accelerators Conference, Portland, OR, May 12–16, 2003.
[3] B. Barstow, M. Liepe, H. Padamsee, Engineering a light source for the future, in: 11th Workshop on RF Superconductivity, SRF 2003, September 8–12, 2003, Lübeck, Germany.
[4] Trans-Tech Inc., http://www.trans-techinc.com
[5] Countis Laboratories, http://www.countis.com
[6] Ceradyne, Inc., http://www.ceradyne.com
[7] http://tesla.desy.de/new_pages/TESLA_Reports/2002/pdf_files/TESLA 2002-13/hom_absorber_dohlus.pdf.
[8] W. Hartung, Ph.D. Thesis, Cornell University, Ithaca, NY, 1996.
[9] V. Shemelin, M. Liepe, H. Padamsee, Characterization of ferrites at low temperature and high frequency, http://conferences.jlab.org/ERL/2005/talks/WG3/WG3_Shemelin_Sun_1400.pdf, Workshop ERL 2005, Newport News, VA, March 19–23, 2005.